WHOLE-BODY IMAGING AND COUNT PROFILING WITH A MODIFIED ANGER CAMERA. II. IMPLEMENTATION EVALUATION

Michael B. D. Cooke and Ervin Kaplan

Veterans Administration Hospital, Hines, Illinois

In the first part of this report we outlined the principle whereby a scintillation camera may be used in a scanning mode by summation of each scintillation event coordinate $x_i y_j$ with the simultaneous position of the detector head having coordinates $X_a Y_b$ relative to some fixed origin. Examples of its clinical application were given. In this paper we detail the design criteria used in implementing the system together with an evaluation of the device and comments on the advantages and disadvantages of this type of system.

The design aim was to produce an accessory for an existing scintillation camera installation (Picker Dynacamera) which would permit the generation of whole-body images and take full advantage of the existing detection, processing, and magnetic tape storage facilities already available on the camera. The system consists of four basic components. These are (A) a scanning table, motor driven in two rectangular axes; (B) a controller to automatically program table motion; (C) interface electronics for whole-body image formation; and (D) existing Dynacamera installation with videotape recording.

MATERIALS AND METHODS

The scanning table. When the camera is used in a scanning mode, it is necessary for all points on the patient to pass completely under or over the active image zone of the crystal. In our system this is a square of side L equal to 60 matrix points in the final image or 60 × 3 mm in the object, i.e., 18 cm (7 in.). A patient of height h can be wholly imaged longitudinally by a traverse of L + h. This is shown diagrammatically in Fig. 1. Similarly in the transverse axis a patient of width w requires a traverse of L + w.

The scanning table permits a patient to be moved for a total traverse of 211 cm (83 in.) in the longitudinal or X axis and 72 cm (28 in.) in the transverse or Y axis. This permits a patient up to 193 cm (76 in.) to be scanned longitudinally and one up to 54 cm (21 in.) broad to be scanned transversely. A patient up to 72 cm (28 in.) broad can be accommodated if scanned longitudinally in four adjacent nonoverlapping strips.

The choice of the mechanical construction and drive system of the table was determined by the primary requirements that it be possible to image the whole body of a patient up to the size indicated above and that the camera detector head be placed either above or below the patient. The requirement to place the detector head below the patient with a minimum patient-to-detector separation imposes stringent limitations on the size and location of the drive mechanism to eliminate any possibility of mechanical interference with the detector head.

The table surface supporting the patient is coupled to the table frame by two sets of slides mounted at right angles. Each slide consists of an inner and an outer member separated by two captive ball races. The transverse (Y) motion is driven directly from a dc motor mounted on the table frame via a gear track at one end with a shaft and chain coupling to a similar gear track at the other end. The twin positive drive eliminates skewing between the widely separated ends. The longitudinal (X) drive is

Received Mar. 27, 1972; revision accepted June 28, 1972.

For reprints contact: Ervin Kaplan, Nuclear Medicine Service, Veterans Administration Hospital, Hines, Ill. 60141.

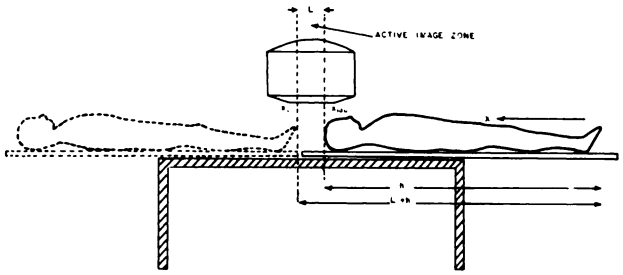

FIG. 1. Longitudinal traverse L + h required to fully image patient of height h using active image zone width L.

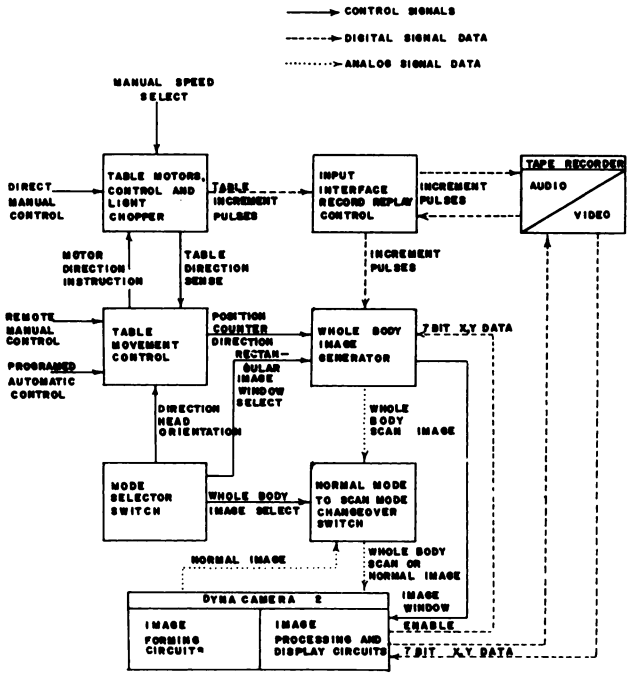

FIG. 2. Electronic interface between scanning table and Dynacamera.

mounted on the Y slides and is driven directly by a second motor via a gear track on one side only. The table surface consists of ⅜-in.-thick Masonite to provide a low-scatter low-cost support when the detector head is positioned below the patient. This system provides stable, firm support and smooth vibration-free motion for all extensions.

Each 3-mm movement of the table corresponding to one matrix interval in the final display generates a pulse from a light chopper directly mounted on the drive shaft of each motor. These pulses are accumulated in a bidirectional binary counter for each axis to generate the coordinates X_aY_b of the table relative to an origin at one of the extreme extensions of the table. The increment pulses are also stored on the two audio tracks of the videotape. On replay both scintillation event x_iy_j coordinates and table X_aY_b coordinates are thus regenerated in the correct time relationship for summation to recreate the whole-body image (Fig. 2).

The drive for the two directions of motion is provided by two Bodine NSH-12RG Model 553 dc motors used in conjunction with a controller Type ASH201. The controller provides a forward, reverse, and brake control together with a variable speed control. Direct current motors rather than stepping motors were selected to obtain maximum torque in the smallest volume and at low cost.

A usefully reproducible speed ratio of 8:1 is obtainable by working on the least steep section of the control characteristic. Table speed ranges from 0.45 cm/sec to 3.6 cm/sec. The lowest speed corresponds to an equivalent static exposure of 40 sec, while the top speed permits positioning from the central rest position to the furthest limit in 30 sec. Table speed on successive traverses is reproducible to within 5% while addition of a 200-lb distributed load produced no significant change.

The controllers have been modified to accept a four line drive signal permitting remote manual or automatic programming of the four directions of motion and braking.

Automatic controller. Thumbwheel switches are used to select the starting point of each scan, scan limits, number of scan strips, and the increment between strips. Scanning in the longitudinal or transverse axis can be selected. Additional exposure is obtained by repeating the scan sequence in reverse. This method may also be used where the isotope decay is significant during the total scan time. Assuming the decay to be approximately linear during the scan, reversal will average out the effects of decay over the whole scan area.

The whole scan can be completed without interference from the operator. Subsequent replay from tape using the same controller settings permits unattended regeneration of images and profiles.

Electronic interface. The interfacing problem is simplified by the fact that the Dynacamera circuitry is divided into an image forming section and an image processing section as shown in Fig. 2.

This circuit organization makes it possible to externally generate the sums $X_a + x_i$ and $Y_b + y_j$ digitally to form X_iY_j and then to convert these to analog signals whose sense, magnitude, and output impedance match those generated within the scintillation camera. These signals are then injected into the scintillation camera in place of the normal x_iy_j analog signals. The processing circuitry now operates on analog signals of similar magnitude but carrying more information, potentially that of a whole-body image when the full X_iY_j matrix is displayed on the oscilloscope or when a whole-body count profile resolved into 100 points is displayed on the data processor.

A scaling amplifier with switched gain selects image display size with scale factors of ⅙, ¼, ½, ¾, and 1 relative to the normal static display. Backing off controls permit examination of any region of the body with less minification. While the use of digital summation is not essential, precision is more easily maintained than with analog summation.

The use of digital electronic selection of the image-forming square is convenient as it avoids the necessity to physically mask collimators with lead.

However, if positional nonlinearity exists in the image it is possible to include points which would have been geometrically rejected by a physical mask and vice versa. This effect has not caused problems in practice.

Exposure schemes. In any exposure scheme the total time required to complete a procedure is composed of a time during which useful data are acquired and a time during which the detector head is moved to a new position without acquiring useful data.

The data contained in any one image point may be generated by scintillation events occurring in one or several positions in the detector crystal depending on the exposure scheme selected.

In the normal static mode of imaging, each image point is generated from scintillations occurring in one small region of the detector crystal; the image resulting from a flood field source is nonuniform. If a whole-body image is generated by a series of static images electronically abutted, then each image has nonuniformity within itself.

Continuous scanning in one direction results in each image point being generated by a continuous line across the crystal in the direction of scan, resulting in a uniformity correction by averaging along that line. The degree of correction is discussed later. The whole body may be imaged by scanning a series of adjacent strips in which case there is no uniformity correction at right angles to the direction of scan. A useful degree of uniformity correction can be introduced by overlapping successive strips. After each continuously scanned strip, the table may be incremented by $\Delta = 30$, 20, or 15 matrix increments at right angles to the scan axis instead of the 60 increments used for adjacent strips. The scan speed is increased by a factor of 2, 3, or 4, respectively, to preserve the same total exposure time. Each point in the final image is now generated by 2, 3, or 4 equispaced lines across the crystal face parallel to the direction of scan. Uniformity is considerably improved when four lines are used and approaches that of the continuous scan.

Continuous scanning has the added advantage of simpler control while the patient is only subjected to a change of motion at the end of each traverse. Information is acquired continuously except during transverse motion between scan strips. In a series of static images no information is collected each time the table increments its position but the total traverse is only h rather than the h + L required for a scan (Fig. 1).

It can be shown that the scan method is quicker when

$$\frac{h}{L} > \frac{1}{k} + 1,$$

where $k = V/U$ and V is the scan velocity determined by the exposure required, while U is the maximum table velocity used for incrementing determined by patient comfort. In our system the minimum value of k is ⅛. In the longitudinal direction, scanning is always the more rapid method ($h/L = 10$ for a 6-ft-tall patient). In the transverse axis where $h/L = 4$ the result is dependent on the value of V.

When successive scan strips are overlapped to improve transverse uniformity there are of course regions of incomplete imaging at the sides. Additional scan strips must be made to insure that the patient lies within the region of complete imaging. The additional time taken is the penalty for improved uniformity.

Table 1 gives a comparative selection of values of total scan time for various degrees of overlap ΔY and patient widths w for an equivalent exposure time $t = 40$ sec with $h/L = 10$ and $k = ¼$.

TABLE 1. SOME COMPARATIVE VALUES OF SCAN TIME T_{TOTAL} FOR VARIOUS VALUES OF ΔY AND w WITH t = 40 SEC, k = ¼, AND h/L = 10

ΔY (matrix units)	w (matrix units)	w (in.)	n (scan strips)	T_{TOTAL} (min)
60	240	28.3	4	29.8
30	240*	28.3*	9*	33.7
20	220*	26.0*	13*	32.5
15	210*	24.8*	17*	31.9
30	210	24.8	8	29.9
60	180	21.3	3	22.3
15	180	21.3	15	28.1

* These are maximum limiting values for the corresponding value of ΔY.

Uniformity and resolution. It has been indicated that image uniformity is improved when several points on the crystal contribute to each point in the final image. This uniformity improvement is greatest along the line of scanning.

The improvement in uniformity is accompanied by a loss of resolution from two causes. While the scan is continuous, the matrix is only incremented every 3 mm; this contributes a small uncertainty in position. This is negligible since the main interest is in examining distribution of isotope over extended areas. A more important contribution to loss of resolution is the nonlinearity within the central image-forming square. Different regions in the image-forming square will place their contributions to the same part of the image in slightly different locations in the final matrix. This causes loss of resolution in the final image in the direction of scan at points

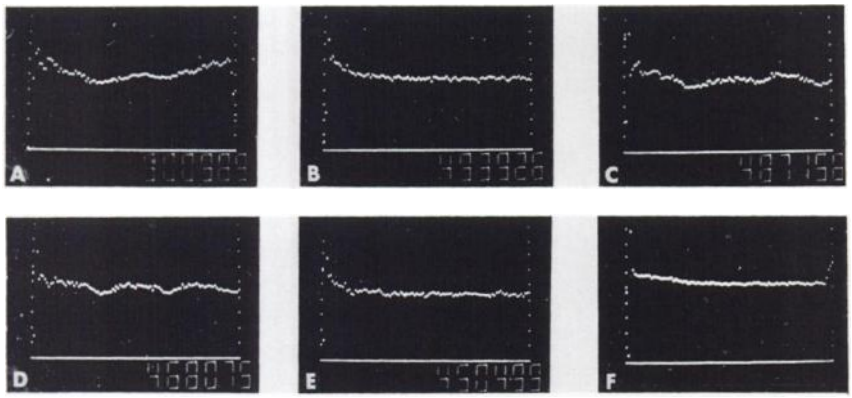

FIG. 3. Profiles of line source taken along its length at scale factor X1: A, normal static camera profile; B, continuous scan along length of line source; C, successive static images abutted $\Delta Y = 60$; D, static images overlapped along line of scan $\Delta Y = 30$; E, $\Delta Y = 15$; and F, x position data replaced by linear analog ramp to show nonlinearities in lower channels of data processor.

where there is appreciable change in linearity across the image-forming square, such as the opposite sides of a barrel distortion. While there may be advantages in setting up the scintillation camera to optimize on linearity at the expense of uniformity no attempt to do this has been made since the aim of the scanning modification is to avoid any alteration of the existing normal functioning of the camera.

The improvement in uniformity resulting from scanning and different degrees of overlap of adjacent images is illustrated in Fig. 3A–E. Each figure represents a profile of the distribution of ^{99m}Tc evenly distributed in a glass tube 1.25 in. diam lying along a diameter of the detector head parallel to the direction of motion. In each case the tube lies within 0.25 in. of the surface of the low-energy collimator. A total integrated exposure of 100 sec is used for the static profiles and a nearly equivalent exposure for the scanned profile. All measurements are made at $\times 1$ scale factor; the same section in the center of the source tube and the same area of detector crystal are used in each case.

Figure 3A is the profile obtained from the whole diameter of the detector with the camera in its normal static mode of use. Figure 3B is the profile generated when a continuous scan is made along the length of the tube to give maximum uniformity improvement in that direction. Figure 3C–E is generated by making a series of static exposures using the central 60 $\times$ 60 image square. The table is advanced by 60, 30, and 15 matrix increments, respectively, between successive exposures. For comparative purposes the movement is made along the same crystal axis as the continuous scan but the intention is to demonstrate the uniformity improvement which can be expected in the direction at right angles to the line of scan when adjacent strips are abutted or overlapped by different increments. Quantitative comparisons of the profiles are made below.

An increased counting rate in the lower channels is particularly evident in Fig. 3B and E. It is suspected that this is caused by nonlinearity in the data processor. The profile in Fig. 3F was produced by using the fixed-frequency internal test signal of the camera to generate y-position and z-event information but replacing the x-position signal with an analog ramp voltage from a function generator. This is injected in place of the x component of the whole-body image signal, Fig. 2. The ramp voltage has the same amplitude p-p as the normal analog signal representing the full image width and so the camera test signal can be swept across all 100 channels of the data processor. This procedure should generate a profile parallel to the baseline. The degree of nonlinearity displayed in Fig. 3F is similar to that observed in Fig. 3B and E. It would thus appear that the nonlinearity is introduced either at the output end of the camera or more likely in the data processor. This problem is being further investigated but does not appear to be caused by the scanning modification.

A quantitative assessment of the uniformity improvement was made by comparing the observed relative standard deviation from the mean count for the top 50 channels of each profile Fig. 3B–E and the central 60 channels of profile Fig. 3a. The central 60 channels of the static profile Fig. 3A correspond to that part of the detector contributing to profiles Fig. 3B–E. The top 50 channels were selected in the other profiles to avoid the artifact in the lower channels discussed above.

The results are given in Table 2. This shows that with successive overlaps of 15 matrix points the relative standard deviation which is used as an index of uniformity approaches that of a continuous scan which in turn is only slightly greater than the value expected from counting statistics.

Image resolution was compared for images obtained statically and in the scanning mode by making comparative exposures of the image obtained from two parallel line sources of various separations. Each line source consisted of a plastic tube 0.022 in. i.d. containing $^{99m}TcO_4^-$. The line sources were mounted <0.2 in. from the face of the low-

TABLE 2. QUANTITATIVE UNIFORMITY IMPROVEMENT MEASURED BY RELATIVE STANDARD DEVIATION FOR EXPOSURE SCHEMES USED IN FIG. 3

Mode of imaging	Fig. 3 profile	Observed relative % s.d.	Relative % s.d. due to counting statistics
Single static image	a	4.84	1.44
$\Delta = 60$	c	4.26	1.44
$\Delta = 30$	d	3.49	1.47
$\Delta = 15$	e	1.76	1.49
Continuous scan	b	1.66	1.45

energy collimator at right angles to the scan axis. Exposures were made at $\times 1$ image scale factor with the camera (A) in its normal static mode of use, (B) using the scanning electronics but without scanning, and (C) in the scanning mode with a single pass. In addition, exposures with scale factors of $\times ½$, $\times ¼$ and $\times ⅙$ were made in the scanning mode.

In the static mode the lines were resolvable at 0.625 in. (15.9 mm) separation but not at 0.5 in. (12.7 mm). No difference was observable between the images obtained by methods A and B at $\times 1$ scale factor indicating that the scanning electronics caused no reduction in image quality. Comparison of methods B and C showed that in C the lines were unresolved at one end which was attributable to a more severe barrel distortion at one side of the image-forming square, causing loss of resolution in the scan mode. On increasing the line separation to 0.75 in. (19–0 mm) the lines were resolved across the full width of the scan image. No loss of resolution was observed at reduced scale factors showing that the spot size of the oscilloscope was not a limiting factor, however, $\times ⅙$ appeared to be the lower limit.

SUMMARY

We have demonstrated that the utility of an existing scintillation camera system can be extended to whole-body imaging and count profiling of static distributions of radioisotope by an add-on accessory while retaining the use of existing parallel-hole collimators.

Image quality is satisfactory but dependent on good positional linearity within the area of detector used. Selective tuning to improve positional linearity or to extend the region of adequate linearity would increase the resolution or the sensitivity, respectively, in an Anger system. Delay-line cameras with improved position arithmetics (*1*) may realize better use of the crystal area.

Uniformity is improved along the line of scan while in the transverse axis it may be improved by overlap scanning but with the penalty of increased total scan time.

ACKNOWLEDGMENTS

We wish to thank Picker Corporation, Medical Manufacturing Division, for their cooperation in this project. The scanning table was designed in consultation with and manufactured by Gamma Products, Inc., Chicago.

REFERENCE

1. NOHARA N, TANAKA E, HIRAMOTO T: High-resolution scinticamera based on delay-line time conversion. *J Nucl Med* 12: 635–636, 1972